
Masters Theses

Student Theses and Dissertations

1959

A cell-center distribution function for liquid argon

Arthur M. Soellner

Follow this and additional works at: https://scholarsmine.mst.edu/masters_theses

 Part of the [Physics Commons](#)

Department:

Recommended Citation

Soellner, Arthur M., "A cell-center distribution function for liquid argon" (1959). *Masters Theses*. 5552.
https://scholarsmine.mst.edu/masters_theses/5552

This thesis is brought to you by Scholars' Mine, a service of the Missouri S&T Library and Learning Resources. This work is protected by U. S. Copyright Law. Unauthorized use including reproduction for redistribution requires the permission of the copyright holder. For more information, please contact scholarsmine@mst.edu.

T 1221
c. 1

R 3606-E20

A CELL-CENTER DISTRIBUTION FUNCTION
FOR LIQUID ARGON

BY
ARTHUR M. SOELLNER

A
THESIS

submitted to the faculty of the
SCHOOL OF MINES AND METALLURGY OF THE UNIVERSITY OF MISSOURI
in partial fulfillment of the work required for the

Degree of
MASTER OF SCIENCE, PHYSICS MAJOR

Rolla, Missouri

1959

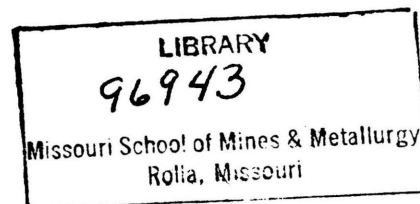
Approved by

Louis W. Gurd. (advisor)

S. J. Pagano

Harold Q. Tuller

Roger E. Nolte



ACKNOWLEDGEMENT

The writer wishes to express his sincere appreciation for the active interest and guidance extended to him throughout the course of this investigation by Dr. Louis H. Lund, Professor of Physics at the University of Missouri School of Mines and Metallurgy, Rolla, Missouri.

CONTENTS

| | |
|-----------------------------------|----|
| Acknowledgement | ii |
| List of Illustrations | iv |
| List of Tables | v |
| Introduction | 1 |
| Review of Literature | 5 |
| Discussion | 9 |
| Theory | 11 |
| Application of Theory | 16 |
| Results and Conclusions | 32 |
| Summary | 35 |
| Bibliography | 36 |
| Vita | 38 |

LIST OF ILLUSTRATIONS

| Figure | Page |
|---|------|
| 1. Atomic cells of two neighboring atoms | 12 |
| 2. Temperature-pressure diagram for argon with datum points corresponding to x-ray scattering patterns . | 17 |
| 3. Graphical representation of the function $X^2(ka)$. . | 18 |
| 4. Increase of cell size with temperature | 19 |
| 5. Atomic and cell-center density distribution functions for liquid argon at 84.4°K | 21 |
| 6. Atomic and cell-center density distribution functions for liquid argon at 91.8°K | 22 |
| 7. Atomic and cell-center density distribution functions for liquid argon at 126.7°K | 23 |
| 8. Atomic and cell-center density distribution functions for liquid argon at 144.1°K | 24 |
| 9. Atomic and cell-center density distribution functions for liquid argon at 149.3°K | 25 |
| 10. Atomic and cell-center density distribution functions for argon gas at 149.3°K | 26 |
| 11. Discontinuity caused by occurrence of a zero in $X^2(ka)$ function in denominator of Equation 14 . . . | 27 |
| 12. Atomic and cell-center distribution functions for liquid argon at 84.4°K | 29 |
| 13. Atomic and cell-center distribution functions for liquid argon at 91.8°K | 30 |

LIST OF TABLES

| Number | Page |
|---|------|
| 1. Positions and co-ordination numbers of atomic concentrations for atomic and cell-center distribution functions | 34 |

INTRODUCTION

The structure of a liquid is not as well defined or as specific as that of a solid or gas. This is especially true in comparison to the crystalline phase of the solid at absolute zero and the perfect gas as a limiting case of a real gas. The liquid more or less forms a bridge between the solid and gaseous phases, and may be regarded either as an imperfect gas in which multiple collisions are frequent or as a distorted crystal in which the long range order has been lost.

Both theories have been advanced with the former being the most satisfactory from a theoretical standpoint, but the crystal-like concept has led to several treatments which can be employed to give numerical results. There are two basic approaches which can be used, the cell theory, which is utilized in this study, and the hole theory.

One of the best methods of describing the structure of a liquid is of a statistical nature in terms of its atomic or molecular distribution function which gives the average number of atoms or molecules between distances R and $R + dR$ from any other arbitrary atom or molecule chosen in the liquid. A curve of this function presents a graphical representation of the time-averaged atomic or molecular arrangements induced under the action of characteristic interatomic or intermolecular forces.

The diffraction of x-rays by liquid elements has

supplied the majority of known distribution curves. Investigation by this method began in 1913 when Friedrich (1) obtained x-ray diffraction patterns of Canadian balsam, paraffin, and amber. In 1916, Debye and Scherrer (2) obtained diffraction patterns of benzene and various other liquids. Then in 1922, Keesom and de Smedt (3) carried out work of a similar nature with nitrogen, oxygen, and argon in the liquid state, which provided qualitative information regarding the structure of these elements.

Theoretical investigations made by Zernicke and Prins (4) and by Debye and Menke (5) supplemented the previous experimental work. Zernicke and Prins introduced the idea of an atomic or molecular distribution function, which if known for a particular substance, would allow the diffraction pattern for the substance to be obtained. They also suggested that the reverse of the above was true, that if the experimental data is known exactly, then the distribution function can be determined from the experimental curves. Debye and Menke completed theoretical work on this method and applied it to liquid mercury.

The combined experiment and theory has led to the determination of atomic distribution in liquids, which in turn has provided valuable information describing the structure of a liquid. Gingrich (6), in his paper, has introduced a satisfactory theoretical approach developed by

1. All references are in bibliography.

Warren and Gingrich (7) and by Warren (8) to the subject of x-ray diffraction and presents a summary of the experimental investigations carried out on twenty-three elements in the liquid state.

The most extensive work has been performed with liquid argon because it is closely representative of hard sphere molecules, its atomic structure factor is known, and its critical temperature and critical pressure are known and can be reached fairly easily. Eisenstein (9) undertook the task of obtaining x-ray scattering patterns by argon using twenty-six different combinations of temperature and pressure. Six of the resulting distribution curves can be found in an article by Eisenstein and Gingrich (10), and it is these particular combinations of temperature and pressure with which this study will also be concerned.

Neutron diffraction studies have presented the most recent advances in determining liquid structures. In 1949, Chamberlain (11) investigated the neutron diffraction patterns of the elements sulfur, lead, and bismuth in the liquid state. In 1952, Sharrah and Smith (12) carried out further study of atomic distribution in liquid lead and liquid bismuth at two temperatures. In 1953, Henshaw, Hurst, and Pope (13) investigated the structures of liquid nitrogen, oxygen, and argon by neutron diffraction. Henshaw (14) remeasured the scattering from liquid argon with higher statistical accuracy in 1956.

Undoubtedly, the future will lead to more developments

in determining atomic distributions in liquids. Many liquid elements still have not been investigated thoroughly, and for those in which the atomic distribution is known, new and advanced methods should ensure more accurate results. A knowledge of atomic distributions in liquids is of great importance for liquid theory. Besides leading to the description of liquid structures, the knowledge of atomic distribution functions in liquids, coupled with knowledge of the potential function, should be enough to calculate all the thermodynamic properties of a liquid.

REVIEW OF LITERATURE

The free volume theory of liquids is based on a model where a system of N interacting atoms of a liquid are required to remain within the confines of a cell, with one atom per cell. Each atom is free to move around within its own cell and the volume to which it has access is termed its free volume. The distribution function which arises from this type of model differs only in the fact that the atoms are not allowed to move beyond the boundaries of their own cells. The free volume ensures the individual mobility of the atoms to which all liquid bodies owe their fluidity, and is a necessary, though not sufficient, condition for relatively large deviations of the atoms from the regular arrangement characteristic of the crystal structure. An excellent coverage of cell methods and the concept of free volume can be found in the book by Hirschfelder, Curtiss, and Bird (15).

In 1927, Prins and Zernicke (16) first considered the idea of free volume by attempting to reduce the structure diffusion of liquids to their excess volume with respect to the corresponding crystals. They later abandoned this view in favor of a temperature dependence theory.

The first actual free volume theories of the liquid state were developed by Eyring (17) and his co-workers and by Lennard-Jones and Devonshire (18). From these a useful approximate description of the thermodynamic properties of

liquids in terms of intermolecular forces has been provided. A free volume is defined in terms of the Gibbs phase integral in the configuration space of N molecules. The free volume is then calculated without reference to the exact Gibbs theory by reasonably assumed models, in which each molecule is supposed to execute gas-like thermal motion in a cage formed by the inter-molecular force field of its neighbors. These two theories differed only in that in the version advanced by Eyring and his associates the cell volume is somewhat less than the molecular volume so that vacant cells and even possibly doubly occupied cells may occur, while that of Lennard-Jones and Devonshire adjusted the cell volume to the molecular volume, thus eliminating the probability of vacant or doubly occupied cells.

Kirkwood (19) has placed the free volume theory of the liquid state on a firmer and less empirical basis by using a fundamental statistical mechanics approach with well-defined approximations. Spanning the liquid with a virtual lattice of N cells with single cell occupancy, and minimizing the configuration contribution to the Helmholtz free energy, he develops an integral equation for the distribution function for each molecule within its cell. A zeroth-order approximation to the solution then gives the earlier formulation of the cell method of Lennard-Jones and Devonshire.

The work of these pioneers has led to further advances in the study of the cellular free volume theories, a few of

which will be mentioned here. Buehler, Wentorf, Hirschfelder, and Curtiss (20) calculated the exact free volume and equation of state for rigid sphere molecules taking into account the exact geometry imposed by face-centered cubic packing and found that the size and shape are quite different from that of the inscribed spheres which correspond to Lennard-Jones and Devonshire approximations. Salsburg and Kirkwood (21) extended the theory to multicomponent mixtures using the method of moments in the treatment of the order-disorder problem. Prigogine (22) and his associates applied its principle to r -mer molecules for firmer study of r -mer liquids. Green (23) has taken the cell model, and following Kirkwood's method, has introduced a cell-cluster type of model in an attempt to eliminate a few of the inconsistencies remaining in the cell model. Dahler, Hirschfelder, and Thacher (24) have recently introduced approximations which spherically symmetrize the free volume and render Kirkwood's equation suitable for solution on digital computers.

Early work connecting distribution functions with the free volume theory as developed by Eyring, and Lennard-Jones and Devonshire, was also undertaken by Kirkwood (25), who formulated an integral equation for radial distribution functions in liquids. Kirkwood and Boggs (26) applied a general method to obtain an approximate solution for the radial distribution function of a system of hard spheres, which they compared to the experimentally determined distribution curves for liquid argon. Rushbrooke (27) calcu-

lated the shape of the first peak on the distribution curve for liquid argon. Using a theory developed by Wall (28) for calculating the free volume per atom, in which it is assumed a single model of the quasi-solid type in which each atom is trapped by its immediate neighbors in a small spherical cell, Lund (29) obtained theoretical distribution curves for liquid argon at 84.3 °K and 91.8 °K, which he compared to those obtained experimentally by Eisenstein and Gingrich (10). Kerr and Lund (30) developed a radial atomic distribution function involving the interatomic potential function of two atoms in the liquid. The theoretical distribution curve was fitted to the left-hand side of the first peak of the experimental distribution curves of liquid argon and liquid mercury.

Recently, Lund (31) has applied Kirkwood's theory to calculate the x-ray scattering from a free volume liquid, and has introduced the notion of a cell-center distribution function. The x-ray intensity function is averaged over configurations of the atoms in a cellular free volume configuration space corresponding to single cell occupancy. A zeroth-order approximation to the derived scattering equation leads to the conventional x-ray scattering equation.

DISCUSSION

To the present time, the atomic distribution function and resulting atomic distribution curves have presented much of the information necessary for determining liquid structures. Experimental and theoretical investigations have been carried out with numerous liquid elements by various individuals for this purpose. The experimental studies of Eisenstein (9) with liquid argon has presented the most qualitative and comprehensive work on a single liquid element. He investigated twenty-six different combinations of temperature and pressure from which he determined atomic distribution curves for liquid argon at temperatures of 84.4°K , 91.8°K , 126.7°K , 144.1°K , and 149.3°K and argon gas at 149.3°K .

In the development given here, the notion of a cell-center distribution function introduced by Lund (31) shall be exploited to give a comparable picture of the structure of liquid argon. An expression will be developed for a cell-center distribution function using fundamental statistical mechanics principles. From this theoretical expression and experimental intensity data provided in Eisenstein (9), cell-center distribution curves for the same temperatures listed above will be developed. A comparison will be made between the theoretically determined cell-center distribution curves and the experimentally determined atomic distribution curves of Eisenstein. The position and co-

ordination number of the first and second atomic concentrations for liquid argon at 84.4°K and 91.8°K will also be found and compared to the experimentally determined values.

THEORY

For the development of the theory it is necessary to consider a liquid of N identical monatomic atoms irradiated by a monochromatic x-ray beam of wavelength λ having the direction of a unit vector \vec{S}_0 . The coherent part of the electric field scattered in the direction of the unit vector \vec{S} by the N atoms in a particular configuration will then be given by

$$E = f \sum_{n=1}^N e^{i\vec{k} \cdot \vec{r}_n} \quad (1)$$

where

f = atomic structure factor

\vec{r}_n = vector from the origin to the n th atom

$K = 2\pi/\lambda(S-S_0)$

The magnitude of K is given by $(4\pi/\lambda)\sin\theta$ where 2θ is the angle between \vec{S} and \vec{S}_0 . The total scattered intensity from the configuration of N atoms averaged over all $\vec{K} = 2\pi/\lambda(\vec{S}-\vec{S}_0)$ can be shown to be

$$I(k) = f^2 \sum_{n=1}^N \sum_{m=1}^M \frac{\sin kr_{nm}}{kr_{nm}} \quad (2)$$

where r_{nm} is the interatomic distance between atoms n and m .

Approaching the free volume theory of the liquid state from a fundamental statistical mechanics viewpoint, we will span the liquid with a virtual lattice of N cells $\Delta_1 \dots \Delta_n$ with single cell occupancy. Denoting the probability density in configuration space by P_n , we have for the average

of the over-all configuration of the N atoms

$$\langle I(k) \rangle = Nf^2 \left[1 + \int \dots \int \sum_{\mathbf{r}_1} e^{i\mathbf{k} \cdot \mathbf{r}_1} P(\mathbf{r}_1 \dots \mathbf{r}_n) \prod_n d\mathbf{v}_k \right] \quad (3)$$

Making the approximation that the probability density in configuration space may be expressed as a product of functions, each of which is a spherically symmetric function of scalar r and a function of the co-ordinate of only one molecule

$$P(\mathbf{r}_1 \dots \mathbf{r}_n) = \prod_i \phi(r_i) \quad (4)$$

it is found that

$$\langle I(k) \rangle = Nf^2 \left[1 + \int \int \sum_{\mathbf{r}_1} e^{i\mathbf{k} \cdot \mathbf{r}_1} \phi(r_1) \phi(r_L) d\mathbf{v}_1 d\mathbf{v}_L \right] \quad (5)$$

where the \mathbf{r}_{1L} is the position vector of the L th cell with respect to the first and the summation extends from an arbitrary atom in the aggregate labeled 1. This arrangement is depicted in Figure 1.

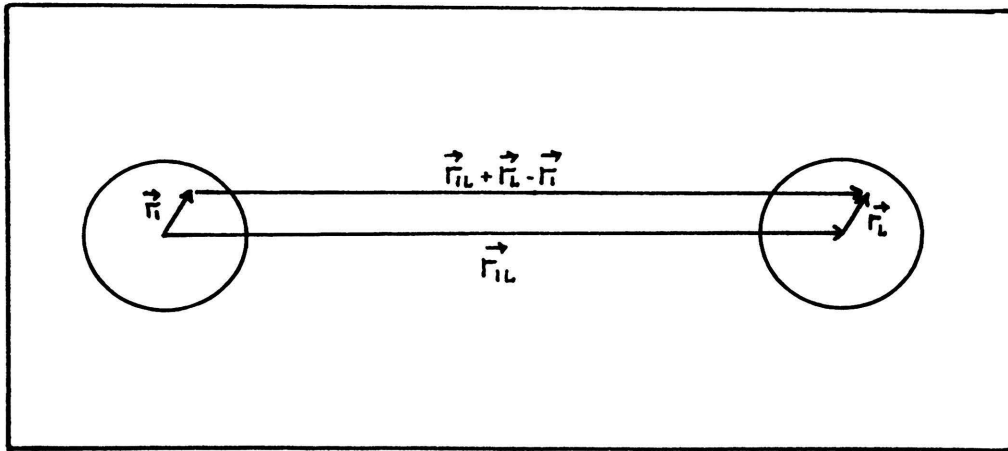


Figure 1. Atomic cells of two neighboring atoms.

It can be seen that the expression on the preceding page can be written as

$$I(k) = Nf^2 \left[1 + \int \int \sum_{L=1}^{\Delta_L} e^{i\vec{k} \cdot (\vec{r}_{1L} + \vec{r}_L - \vec{r}_1)} \phi(r_1) \phi(r_L) dv dv \right] \quad (5)$$

Describing the density of cell-centers about the first cell-center by a function $\rho_c(r_{1L}) = \rho_c(r)$ of the continuously varying $r_{1L} = r$, and also assuming a continuous distribution of atoms, the above summation may be replaced by an integral

$$\langle I(k) \rangle = Nf^2 \left\{ 1 + \int_0^{\Delta} e^{i\vec{k} \cdot \vec{r}} 4\pi r^2 (\rho_c(r) - \rho_0) dr \left[\int_0^{\Delta} e^{i\vec{k} \cdot \vec{r}} \phi(r) dv \right]^2 \right\} \quad (6)$$

where the squared term arises from the fact that the exponents $e^{i\vec{k} \cdot \vec{r}_L}$ and $e^{-i\vec{k} \cdot \vec{r}_1}$ are complex conjugates of each other, and ρ_0 , the average number of equilibrium centers per unit volume, has been introduced into the integrand with subsequent neglect of the ρ_0 contribution of the added compensating integral.

Replacing $\left[\int_0^{\Delta} e^{i\vec{k} \cdot \vec{r}} \phi(r) dv \right]^2$ by $X^2(ka)$ and reducing $e^{i\vec{k} \cdot \vec{r}}$ to the form $\sin kr/kr$ as shown previously in earlier development of the theory, results in the following equation.

$$\langle I(k) \rangle = Nf^2 \left[1 + \int_0^{\Delta} X^2(ka) 4\pi r^2 (\rho_c(r) - \rho_0) \frac{\sin kr}{kr} dr \right] \quad (7)$$

Taking the inverse Fourier transform of the above expression and rearranging, we then have

$$\rho_c(r) = \frac{1}{2\pi^2 r} \int_0^\infty \frac{\left(\frac{\langle I(k) \rangle}{Nf^2} - 1 \right) k \sin kr dk}{X^2(ka)} + \rho_0 \quad (8)$$

The function $X^2(ka)$ is dependent both upon the cell geometry and the probability function $\phi(r)$. Here it is considered that each atom is located within a spherical cell of radius "a", using for a physical model one in which $\phi(r)$ is equal to the reciprocal of the volume inside the cell and zero outside the cell or

$$\begin{aligned} \phi(r) &= 1/v & 0 < r < a \\ \phi(r) &= 0 & a < r < \infty \end{aligned}$$

Having previously defined $X^2(ka)$ as

$$X^2(ka) = \left[\int_0^a e^{i\vec{k} \cdot \vec{r}} \phi(r) dv \right]^2 \quad (9)$$

we now impose the conditions implied by the assumptions made above, giving

$$X^2(ka) = \left[\int_0^a e^{i\vec{k} \cdot \vec{r}} \frac{dv}{v} \right]^2 \quad (10)$$

Since v is the volume with the spherical cell and dv represents a volume element of the cell, we can substitute for these quantities in Equation 10, giving

$$X^2(ka) = \left[\int_0^a \frac{\sin kr}{kr} \frac{3}{r} dr \right]^2 \quad (11)$$

where $e^{ik \cdot r}$ has again been replaced by $\sin kr/kr$. Upon integrating

$$X^2(ka) = \left[\frac{3}{(ak)^3} (ak \cos ak - \sin ak) \right]^2 \quad (12)$$

Substituting the expression for $X^2(ka)$ obtained in Equation 12 into Equation 8, we have

$$\rho_c(r) = \frac{1}{2\pi^2 r} \int_0^\infty \frac{\left(\frac{\langle I(k) \rangle}{Nf^2} - 1 \right) k \sin kr dk}{\left[\frac{3}{(ak)^3} (ak \cos ak - \sin ak) \right]^2} + \rho_0 \quad (13)$$

Since the intensity function $k \left(\frac{\langle I(k) \rangle}{Nf^2} - 1 \right)$ is an experimentally determined quantity and has been obtained over a range K and is zero beyond this point, the limits of integration can be changed and the final working equation, which defines the cell-center density distribution function $\rho_c(r)$, will be

$$\rho_c(r) = \frac{1}{2\pi^2 r} \int_0^{K} \frac{\left(\frac{\langle I(k) \rangle}{Nf^2} - 1 \right) k \sin kr dk}{\left[\frac{3}{(ak)^3} (ak \cos ak - \sin ak) \right]^2} + \rho_0 \quad (14)$$

Another expression which will be used is the cell-center distribution function $4\pi r^2 \rho_c(r)$ given by

$$4\pi r^2 \rho_c(r) = \frac{2r}{\pi} \int_0^K \frac{\left(\frac{\langle I(k) \rangle}{Nf^2} - 1 \right) k \sin kr dk}{\left[\frac{3}{(ak)^3} (ak \cos ak - \sin ak) \right]^2} + 4\pi r^2 \rho_0 \quad (15)$$

APPLICATION OF THEORY

The expression which has been developed on the preceding page forms a basis for determination of cell-center distribution functions in liquid argon using the concept of free volume and locating the atoms in a spherical cell formed by their nearest neighbors. The distribution curves which result from application of this expression are determined at temperatures and pressures shown by datum points 1, 2, 4, 5, 6, and 7 in Figure 2 on the liquid-vapor transition curve. These points correspond to the conditions used by Eisenstein (9) in determining his experimental atomic distribution curves.

It is first necessary to evaluate the function $X^2(ka)$ over a sufficient range in order that Equation 14 may be evaluated. This was done by assuming values for ka in Equation 12 and obtaining a graphical representation of the function as shown in Figure 3. From this graph it is then possible to obtain values of $X^2(ka)$ over the desired range of integration. The radius " a " of the cell was determined by assuming a linear increase of cell size with respect to temperature. Lund (29) has found that the radii of spherical cells for argon at 84.4°K and 91.8°K are 0.37Å and 0.45Å respectively. Using this as a basis of measurement, the remaining radii were approximated using a linear extrapolation. This can be seen in Figure 4. The function $k\left(\frac{\langle I(k) \rangle}{Nf^2} - 1\right)$ has been computed from the experimental inten-

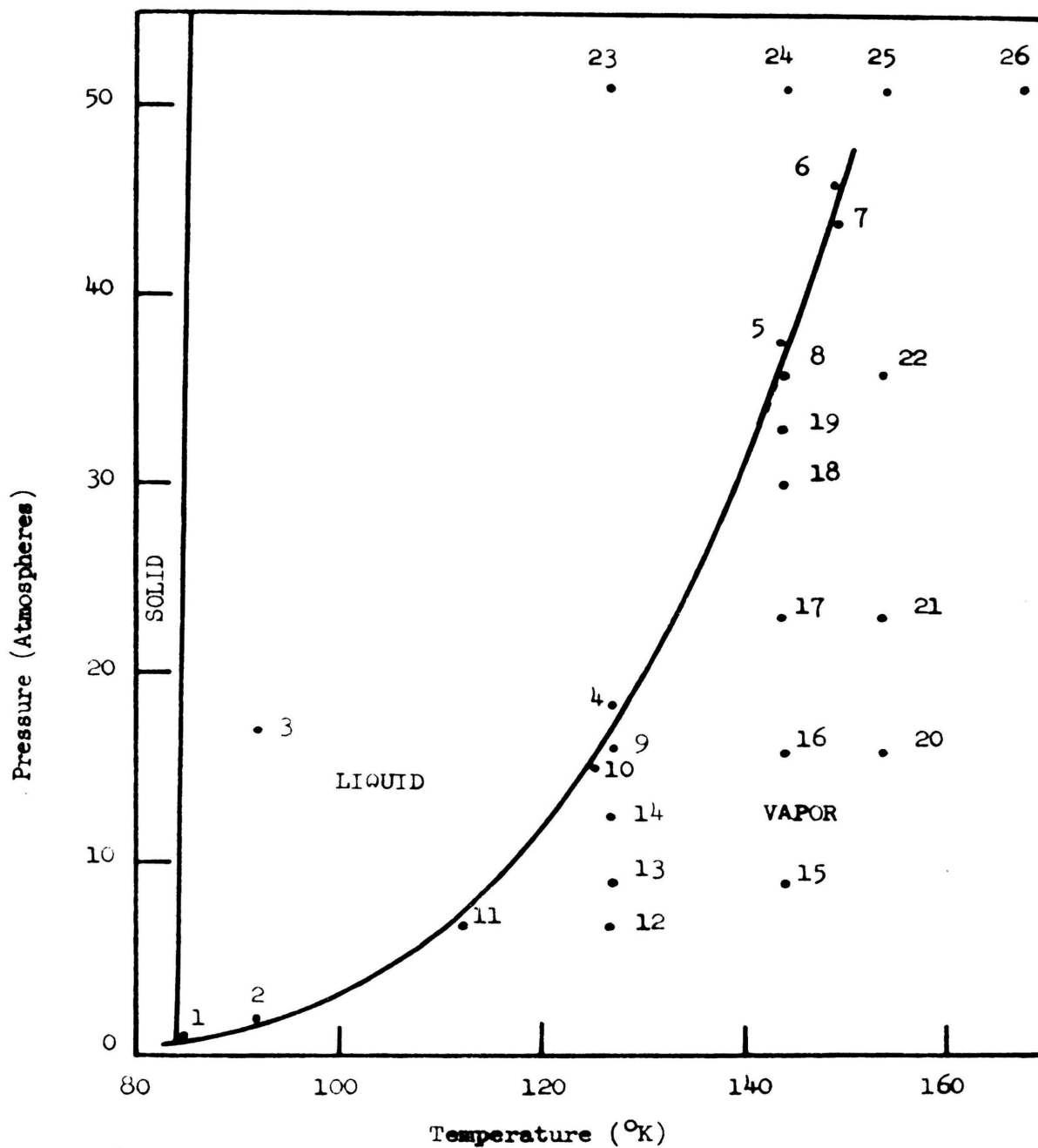


Figure 2. Temperature-pressure diagram for argon with datum points corresponding to x-ray scattering patterns.

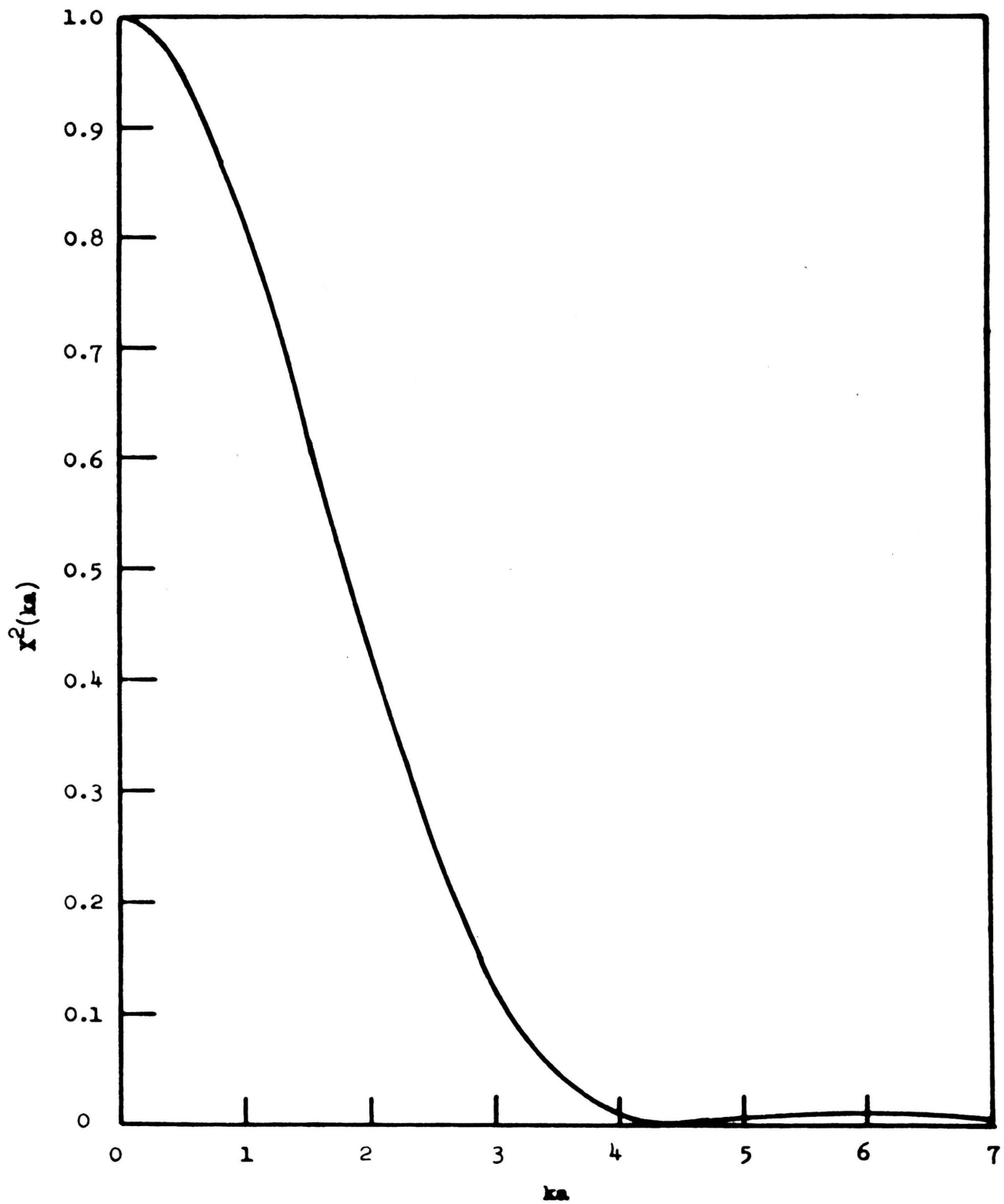


Figure 3. Graphical representation of the function $X^2(ka)$.

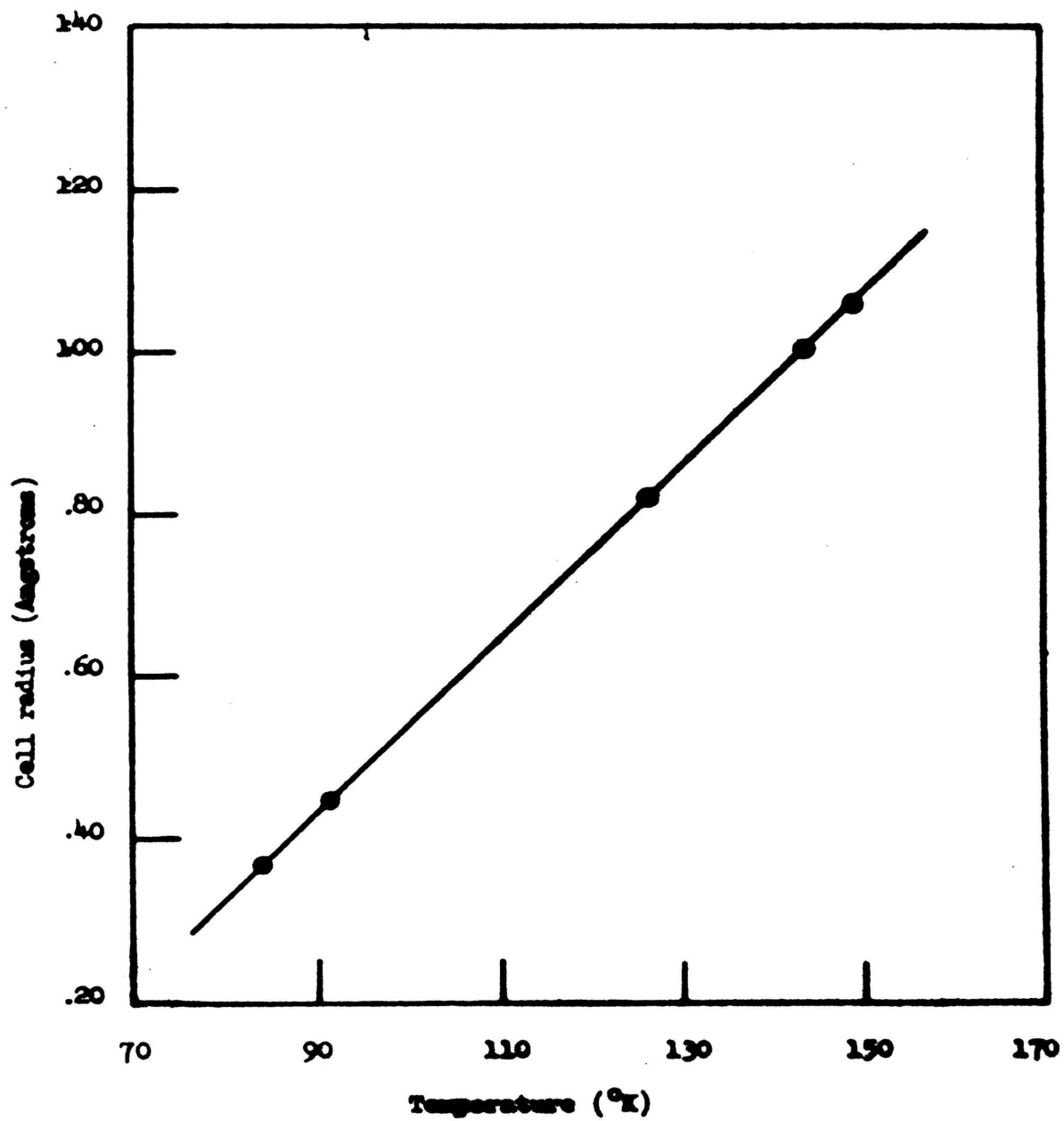


Figure 4. Variation of cell size with temperature.

sity curves and tabulated for various values of $\sin\theta/\lambda = k/4\pi$ by Eisenstein (9).

The cell-center density distribution function curves $\rho_c(r)$ for temperatures of 84.4°K and 91.8°K shown in Figures 5 and 6 were determined by graphical evaluation of Equation 14. Values of r at intervals of 0.25Å were selected over the necessary range of integration, and even smaller intervals of 0.125Å whenever a marked variation in the shape of the curve occurred. Intervals of $k/4\pi$ of 0.01 which corresponds to intervals of k of 0.1256 were used for the graphical evaluation of the integral. Planimetering the area under the curves, the integral was then evaluated over its full range for both temperatures. Multiplying the resulting values by $1/2\pi^2r$ and adding the numerical value of ρ_0 given in Eisenstein (9) for each temperature gives the cell-center distribution curves.

The cell-center density distribution curves for the remaining four temperatures shown in Figures 7, 8, 9, and 10 were also determined by application of Equation 14 but it was necessary to use a modified approach. This comes about because in the expression for $X^2(ka)$, $\tan ak = ak$ at approximately $3\pi/2$ and the function goes to zero at this point. The ranges of k for these temperatures include this point and hence a zero appears in the denominator of Equation 14 which causes an infinite discontinuity in the integral. Since the integral cannot be evaluated graphically a different method must be used.

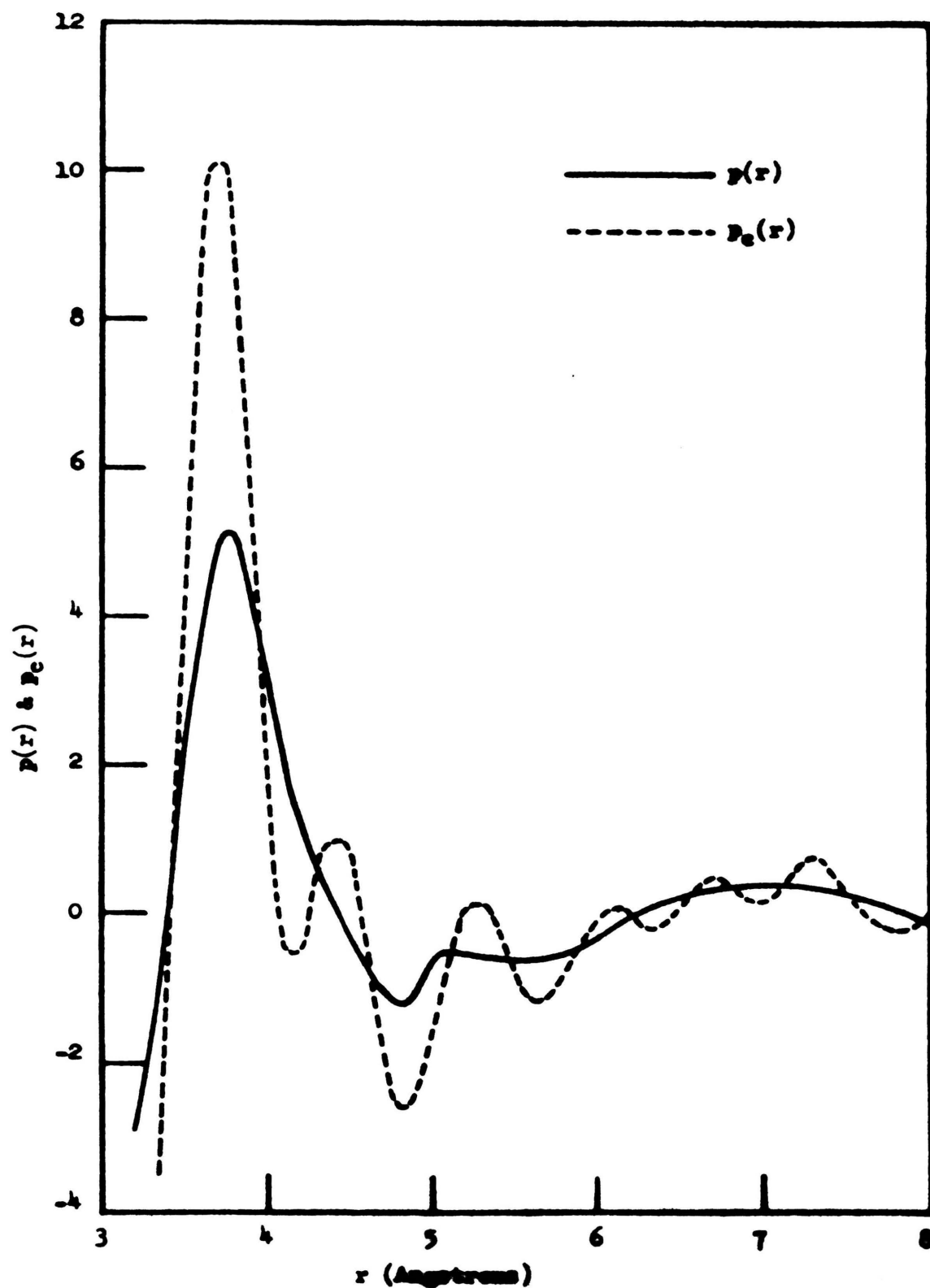


Figure 5. Atomic and cell-center density distribution functions for liquid argon at 84.4 K.

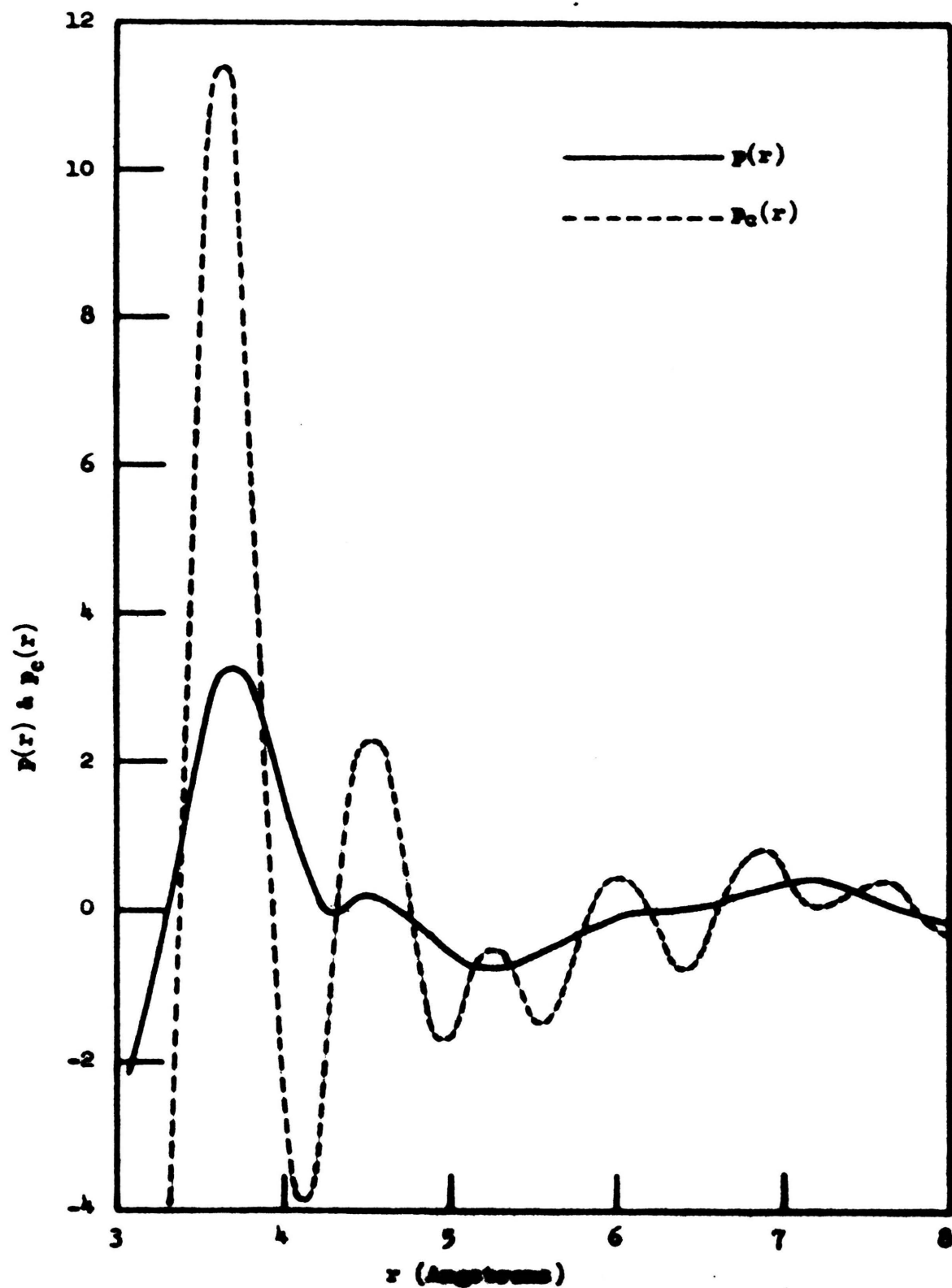


Figure 6. Atomic and cell-center density distribution functions for liquid argon at 91.8 °K.

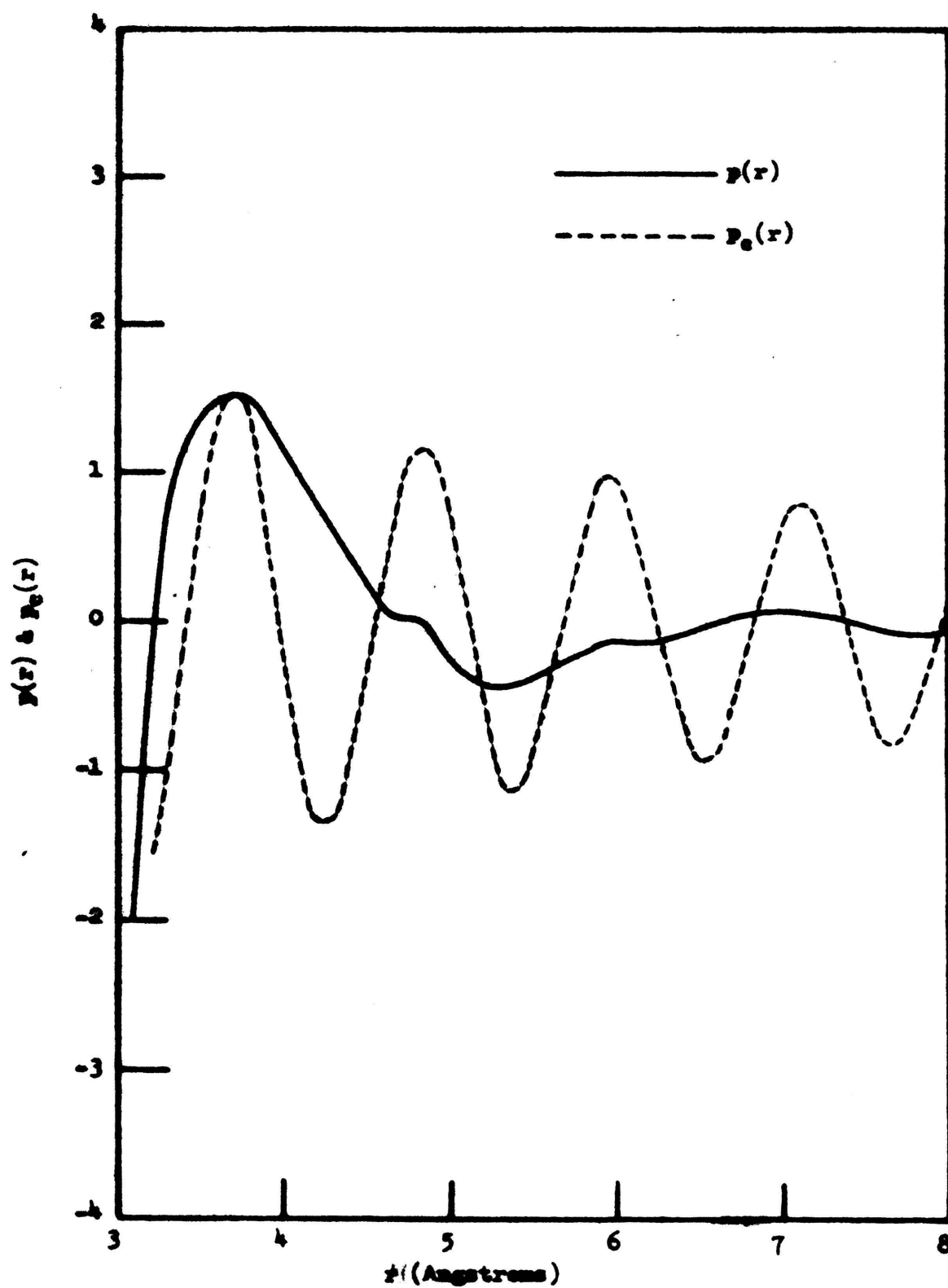


Figure 7. Atomic and cell-center density distribution functions for liquid argon at 126.7 °K.

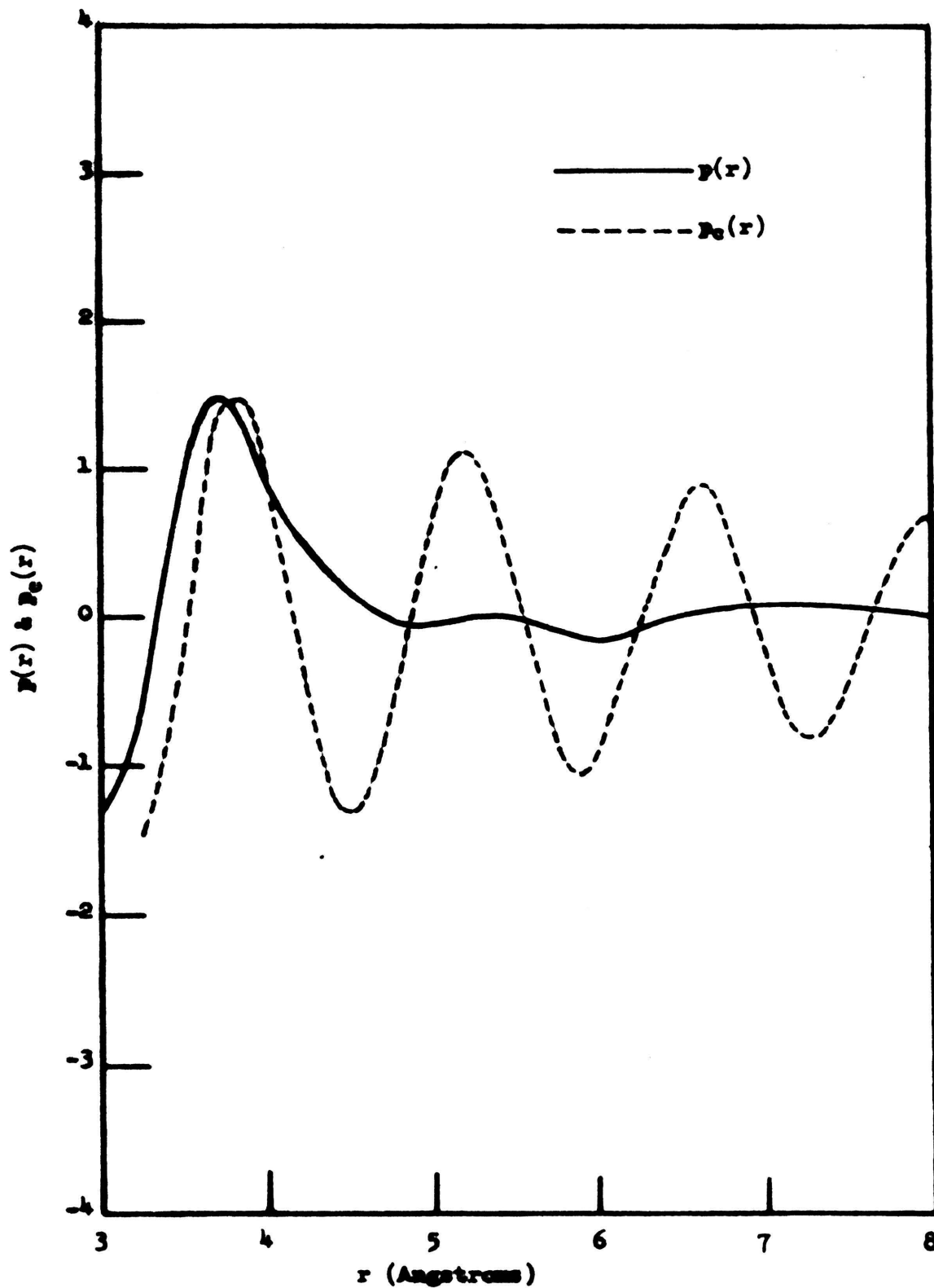


Figure 8. Atomic and cell-center density distribution functions for liquid argon at 144.1 °K.

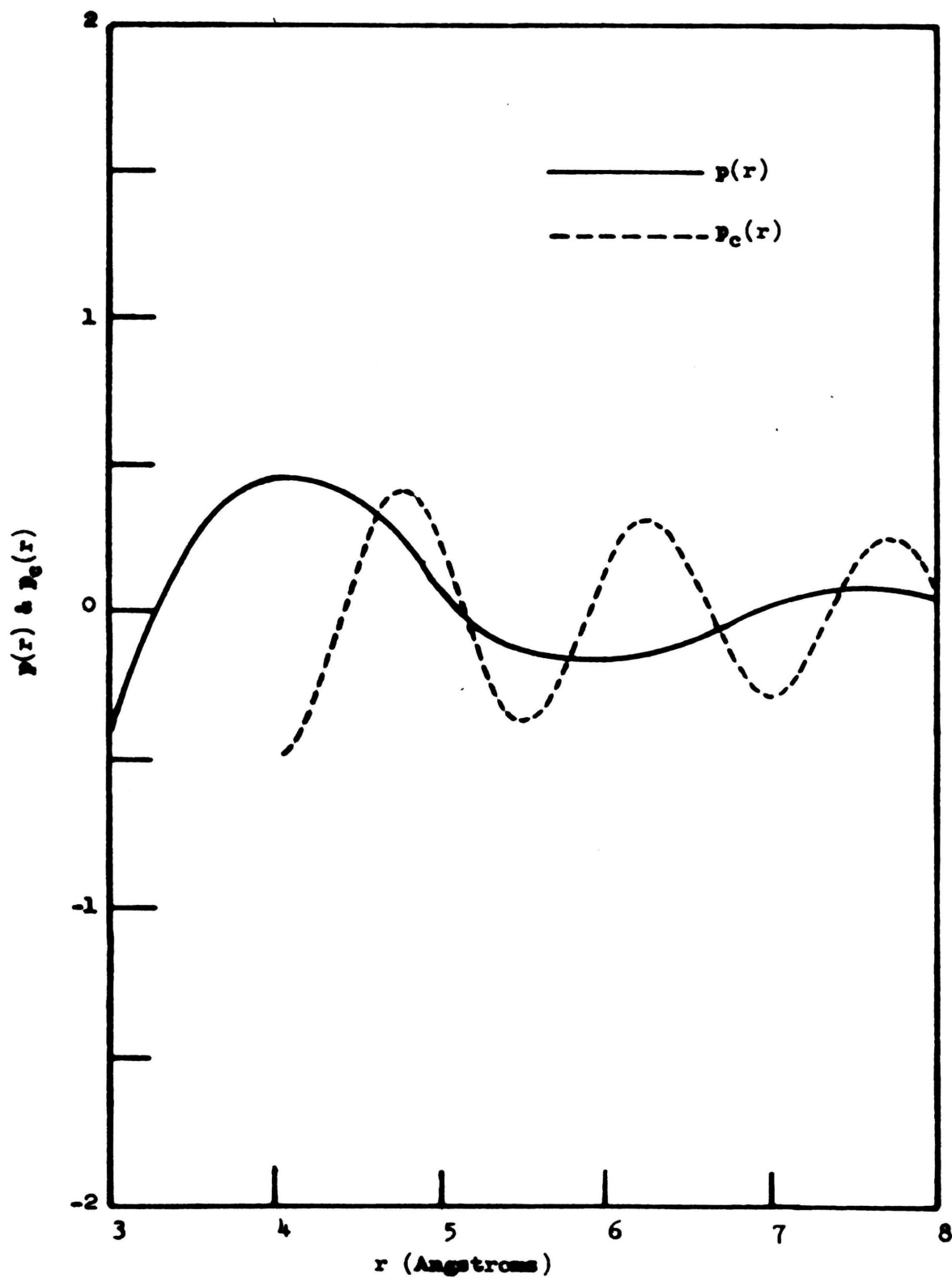


Figure 9. Atomic and cell-center density distribution functions for liquid argon at 149.3 °K.

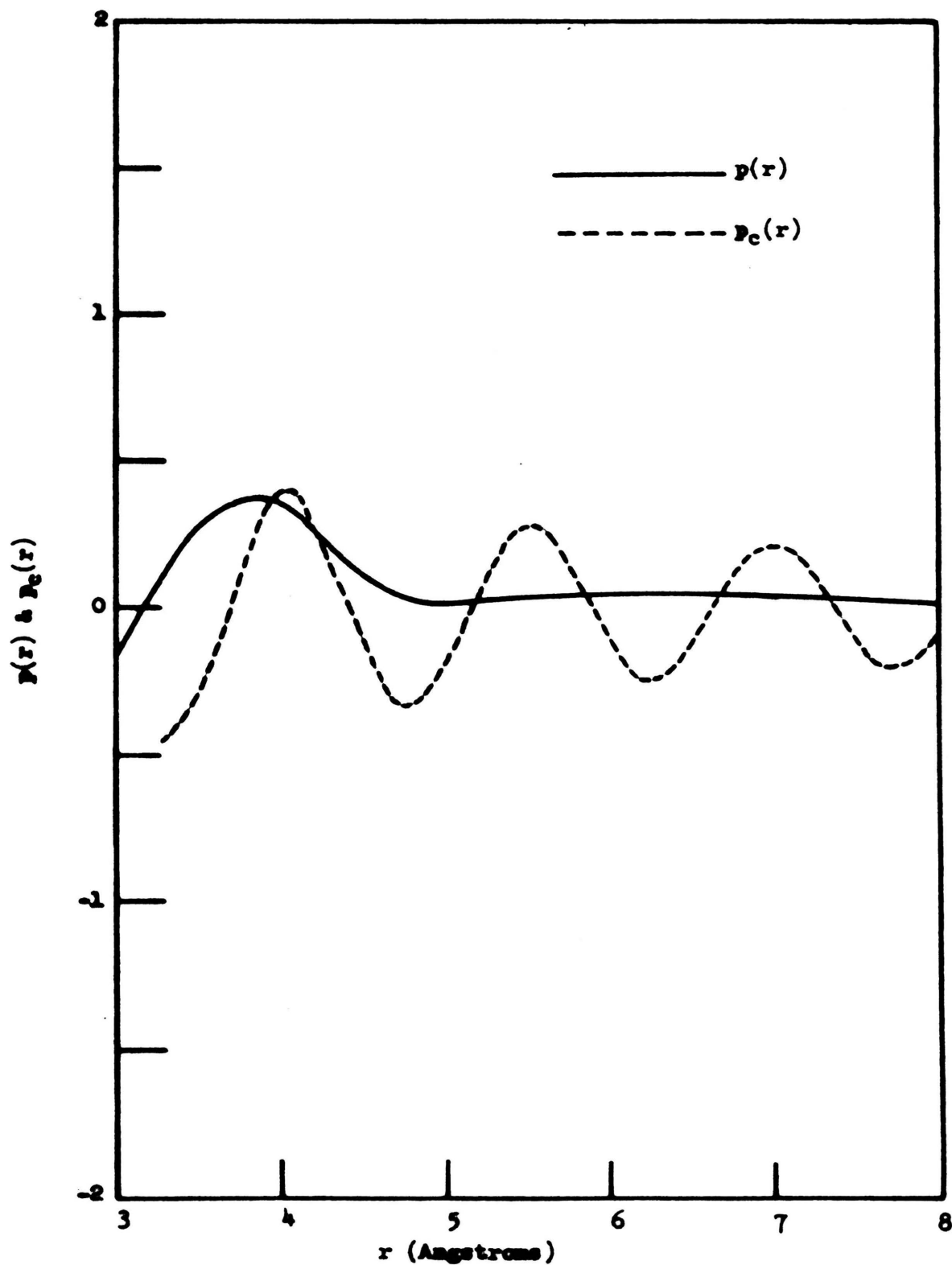


Figure 10. Atomic and cell-center density distribution functions for argon gas at 149.3 °K.

Let Equation 13 be rewritten in the form

$$\rho_c(r) = \frac{1}{2\pi^2 r} \int_0^\infty G(k) \sin kr \, dk + \rho_0 \quad (16)$$

where

$$G(k) = \frac{k \left(\frac{\langle I(k) \rangle}{Nf^2} - 1 \right)}{X^2(ka)} \quad (17)$$

Suppose all the area is considered concentrated between some value $k_0 - \epsilon$ and $k_0 + \epsilon$ with amplitude h at the point k_0 where the infinite discontinuity occurs, as shown in Figure 11.

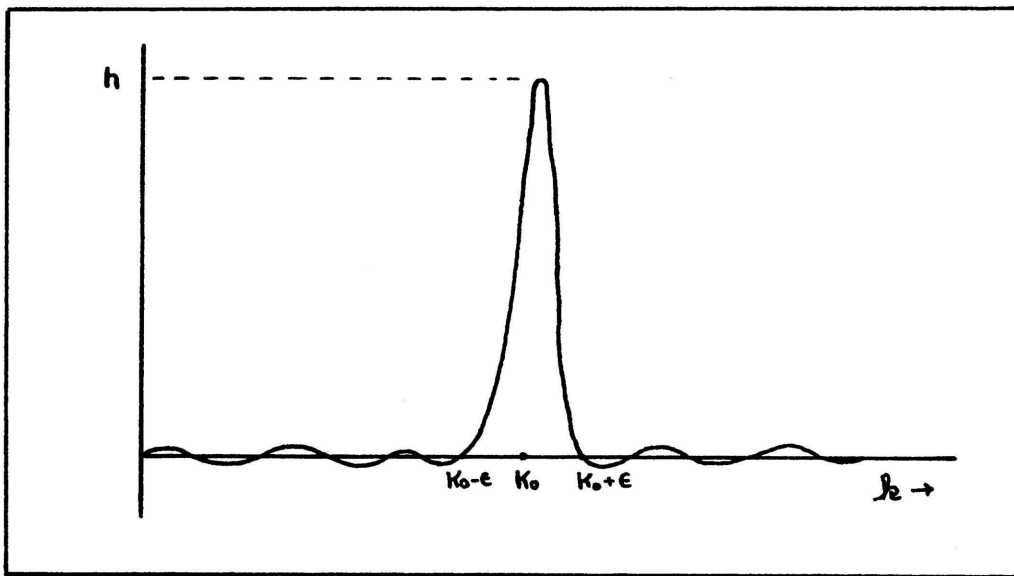


Figure 11. Discontinuity caused by occurrence of a zero in $X^2(ka)$ function in denominator of Equation 14.

If the base is allowed to approach k_0 with h approaching infinity in such a manner that the area remains constant, Equation 16 can be rewritten as

$$\rho_c(r) = \frac{1}{2\pi^2 r} \sin k_0 r \int_0^\infty G(k) dk \quad (17)$$

Under the assumptions that were made, the only place the integral will have a value is at the point $k = k_0$, and this value will be the area under the curve which we will call F . Therefore, the defining equation will now be

$$\rho_c(r) = \frac{1}{2\pi^2 r} F \sin k_0 r + \rho_0 \quad (18)$$

where the numerical value for ρ_0 can again be found in Eisenstein.

Using the above expression, an arbitrary numerical value was given to F for each temperature considered which would match the magnitude of the first peak of the theoretical curves with the first peak of the experimental curves with which they are compared. Representative values of r between 3A and 8A were again used in Equation 18 to evaluate $\rho_c(r)$.

Figures 12 and 13 are graphical representations of the cell-center distribution function $4\pi r^2 \rho_c(r)$ for the temperatures 84.4°K and 91.8°K obtained from evaluation of Equation 15. From this form of the distribution function the areas under the first two peaks of each curve were planimeted to obtain the co-ordination number of the first and second atomic concentrations. The methods used were the same as those by Eisenstein (9) for determination of his

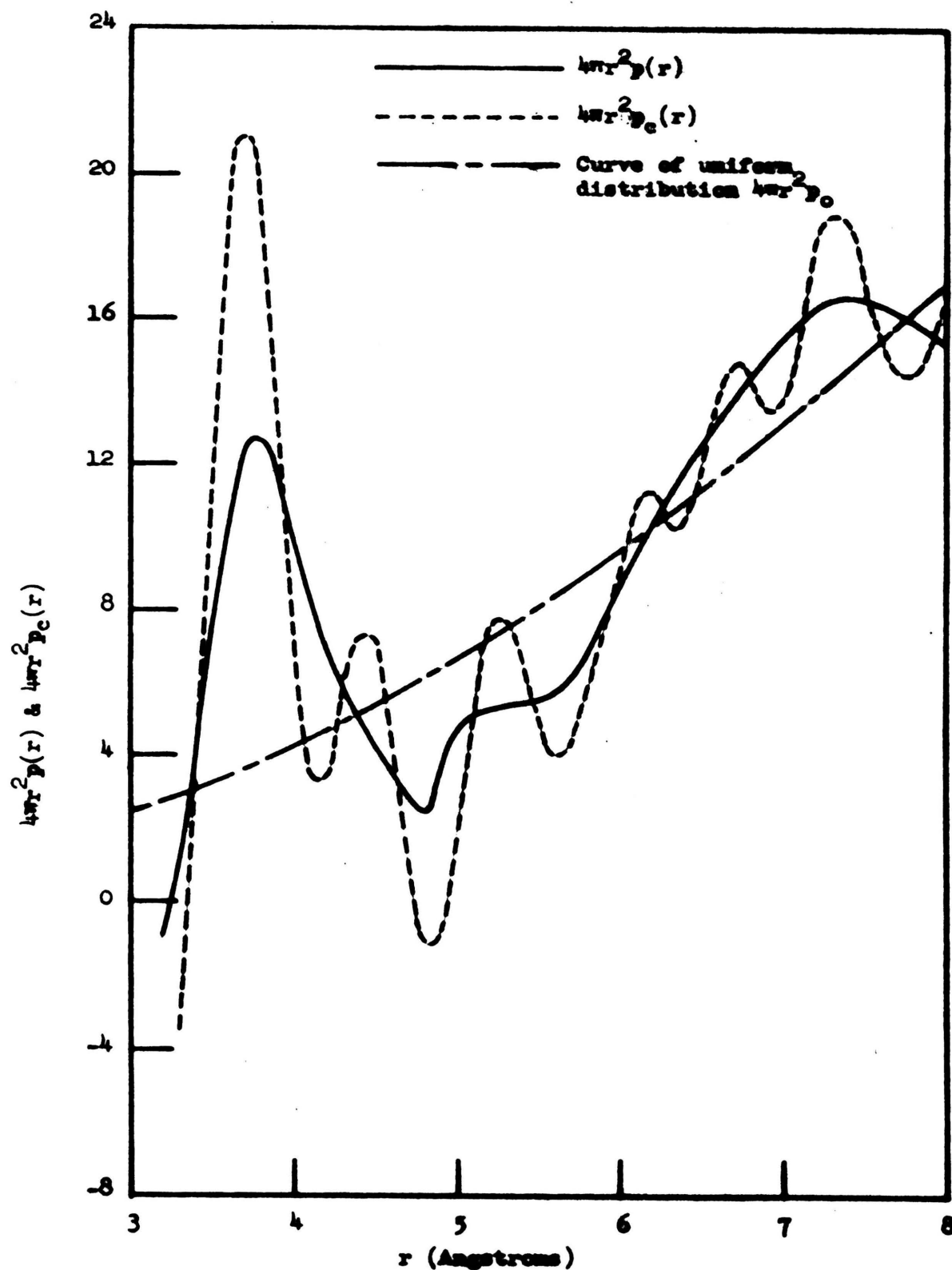


Figure 12. Atomic and cell-center distribution functions for liquid argon at 84.4 °K.

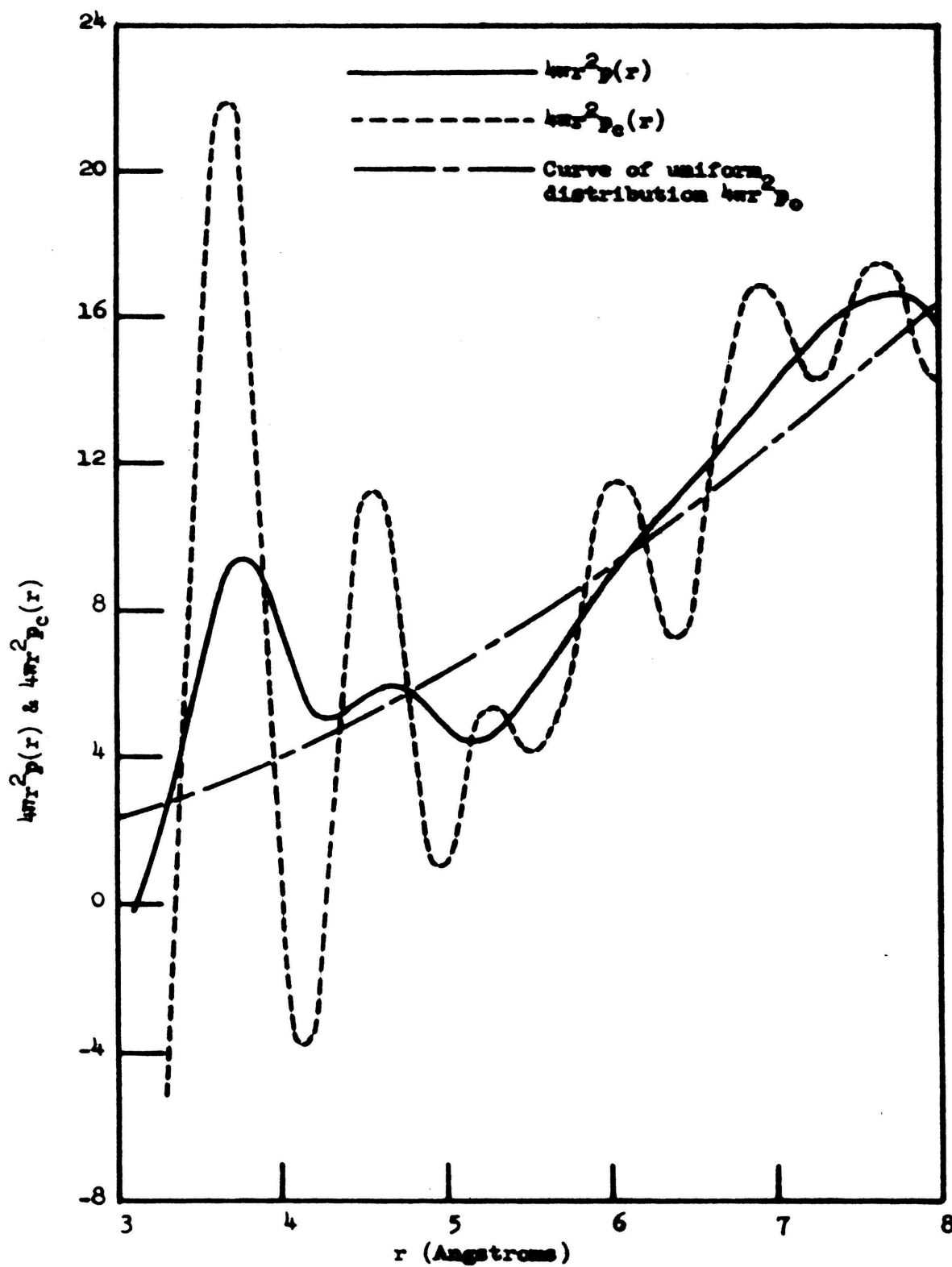


Figure 13. Atomic and cell-center distribution functions for liquid argon at 91.8 °K.

experimental values. Atomic concentrations were obtained first by drawing the curve in symmetric about the peak from which it is desired to determine a value. Secondly, they were obtained by dropping perpendiculars at the minimum points between peaks. Determination of the areas formed by these two methods then gave fairly accurate values for atomic concentrations. The positions at where these peaks occur also gives the location of the atomic concentrations corresponding to the several co-ordination shells.

RESULTS AND CONCLUSIONS

It can be seen from inspection of Figures 5 and 6, which were obtained from application of Equation 14, that the cell-center density distribution curves obtained here are much more sharply defined and more oscillatory than the experimentally determined atomic density distribution curves. The first peaks of the experimental and theoretical distribution curves coincide very well with each other. At other points where peaks occur in the experimental curves, there are corresponding peaks in the theoretical curves. It can also be seen that the theoretical curve oscillates about the experimental curve with the magnitude of the oscillations becoming greater as the temperature is increased. This seems plausible, for an increase in temperature means an increase in cell radius, which necessitates a closer approach to the point of discontinuity of the integral in Equation 14. This causes larger magnitudes of areas which must be planimetered, and hence larger relative magnitudes between the positive and negative areas to give the net area. A physical comparison of the experimental and theoretical distribution curves shows that a more sharply defined and definite structure, much like that expected for a crystal, is predicted using the cell model for a liquid. This can be attributed, to the most part, to the occurrence of the $X^2(ka)$ factor in Equation 14. The experimental distribution curves were obtained from the same expression

less the $X^2(ka)$ factor, the integral being evaluated by the same method of graphical analysis used here. Thus where there are relative large maxima or minima in the expression for the experimental curves, there should be corresponding larger maxima or minima in the expression for the theoretical curves. The $X^2(ka)$, being in the denominator, more or less acts as a multiplicity gain factor, increasing the magnitude of the integral to be evaluated.

Curves for the remaining four temperatures shown in Figures 7, 8, 9, and 10 have all been evaluated over the point of discontinuity and it can be seen that for the assumptions made, distribution curves result which are oscillatory in nature of constant frequency and decreasing amplitude. This could have been predicted from direct observation of Equation 18, for $F/2\pi^2r$ would represent a decreasing amplitude and $\sin k_0r$ a constant sinusoidal frequency term. The theoretically determined curves match fairly well with the experimental curves at the first peak, although there seems to be a distinct shifting of the position of the first peak of the theoretical curves with respect to the experimental curves as the temperature is increased. At values of r past the first peak, any resemblance between the two curves disappears. A physical comparison between the two curves indicates that the cell model predicts a periodic structure with the atomic concentration decreasing in a regular manner with increasing distance from a central cell center. The character of these curves can be attri-

buted to the assumptions made to adjust for the point of discontinuity caused by the $X^2(ka)$ factor.

The atomic concentrations and their positions determined from the cell-center distribution curves $4\pi r^2 \rho_c(r)$ compare fairly well with those predicted by the atomic distribution curves. The table shown below gives the final values obtained here along with those obtained by Eisenstein (9) for his curves. The rows with the asterisks represent the theoretically determined values.

Table 1

| Temperature | First number | Second number | First distance | Second distance |
|-------------|--------------|---------------|----------------|-----------------|
| * 84.4°K | .9.9-10.0 | 3.6-3.8 | 3.70 | 5.25 |
| | 10.2-10.9 | - | 3.79 | 5.3 |
| * 91.8°K | 8.1 | 3.1 | 3.67 | 4.55 |
| | 6.8-7.2 | 3.2-4.7 | 3.79 | 4.7 |

SUMMARY

A theoretical expression for a cell-center distribution function was developed using a fundamental statistical mechanics approach. A free volume picture of the liquid was used with each atom located in a spherical cell formed by its nearest neighbors. Cell-center density distribution curves were obtained for liquid argon for temperatures of 84.4°K, 91.8°K, 126.7°K, 144.1°K, and 149.3°K and for argon gas at 149.3°K, and a comparison made with the experimental atomic distribution curves obtained by Eisenstein (9). For the first two temperatures a sharper, more definite structure was predicted by the cell model. For the remaining four temperatures, with the assumptions made, a periodic structure of regularly decreasing atomic concentrations was predicted. Cell-center distribution curves $4\pi r^2 \rho_c(r)$ were obtained for temperatures of 84.4°K and 91.8°K and the positions and co-ordination numbers of the first and second atomic concentrations were found. A reasonable agreement was found between the values obtained by Eisenstein and those obtained here.

BIBLIOGRAPHY

1. W. Friedrich, Physik. Zeits. 14, 397 (1913).
2. P. Debye and P. Scherrer, Gottingen Nachrichten 16 (1916).
3. W. H. Keesom and J. de Smedt, Proc. Amst. Akad. Sci. 25, 118 (1922); 26, 112 (1923).
4. F. Zernicke and J. Prins, Zeits. Physik. 41, 184 (1927).
5. P. Debye and H. Menke, Ergeb. d. Tech. Rontgenk. II (1931).
6. N. S. Gingrich, Rev. Mod. Phys. 15, 90 (1943).
7. B. E. Warren and N. S. Gingrich, Phy. Rev. 46, 368 (1934).
8. B. E. Warren, J. App. Phy. 8, 645 (1937).
9. A. Eisenstein, PhD. Dissertation, University of Missouri, Columbia, Missouri, June, 1942.
10. A. Eisenstein and N. S. Gingrich, Phy. Rev. 62, 261 (1942).
11. O. Chamberlain, Phy. Rev. 77, 305 (1950).
12. P. C. Sharrah and G. P. Smith, J. Chem. Phy. 21, 228 (1953).
13. D. G. Henshaw, D. G. Hurst, and N. K. Pope, Phy. Rev. 92, 1229 (1953).
14. D. G. Henshaw, Phy. Rev. 105, 976 (1957).
15. J. Hirschfelder, C. Curtiss, and R. Bird, Molecular Theory of Gases and Liquids, New York, Wiley and Sons, (1954).
16. J. Frenkel, Kinetic Theory of Liquids, London, Oxford University Press, (1947).

17. H. Eyring and J. Hirschfelder, J. Phy. Chem. 41, 249 (1937).
18. J. E. Lennard-Jones and A. F. Devonshire, Proc. Roy. Soc. London, 163, 53 (1937).
19. J. G. Kirkwood, J. Chem. Phy. 18, 380 (1950).
20. R. J. Buehler, R. H. Wentorf, J. O. Hirschfelder, and C. F. Curtiss, J. Chem. Phy. 19, 61 (1951).
21. Z. W. Salsburg and J. G. Kirkwood, J. Chem. Phy. 20, 1538 (1952).
22. I. Prigogine, N. Trappeniers, and V. Mathot, J. Chem. Phy. 21, 559 (1953).
23. H. S. Green, J. Chem. Phy. 24, 732 (1956).
24. J. S. Dahler, J. O. Hirschfelder, and H. C. Thacher, J. Chem. Phy. 25, 249 (1956).
25. J. G. Kirkwood, J. Chem. Phy. 7, 919 (1939).
26. J. G. Kirkwood and E. M. Boggs, J. Chem. Phy. 10, 394 (1942).
27. G. S. Rushbrooke, Proc. Roy. Soc. Edinburg 60, 182 (1940).
28. C. N. Wall, Phy. Rev. 54, 1062 (1938).
29. L. H. Lund, J. Chem. Phy. 13, 316 (1945).
30. R. H. Kerr and L. H. Lund, J. Chem. Phy. 19, 50 (1951).
31. L. H. Lund, J. Chem. Phy. 21, 1772 (1953).

VITA

Arthur M. Soellner was born September 24, 1934, in St. Louis, Missouri, the son of Arthur B. and Eunice V. Soellner. He received his elementary education in the public schools of Louisiana and St. Louis, Missouri, receiving a diploma in June, 1947. From September, 1947, to June, 1951, he attended Beaumont High School in St. Louis, receiving a diploma upon graduating in 1951.

In September, 1951, he enrolled at the University of Missouri School of Mines and Metallurgy at Rolla, Missouri, where he received the degree Bachelor of Science, Physics Major in June, 1955. During the year 1953-1954 he worked as a student assistant for the Physics Department.

Upon graduation he accepted employment as an Electronic Engineer at Emerson Electric in St. Louis for a period of fifteen months, during which time he accumulated six hours of graduate study at Washington University in St. Louis. In September, 1956, he transferred to McDonnell Aircraft in St. Louis where he became a member of their Control Dynamics Department. In February, 1957, he enrolled in the graduate school of the School of Mines and Metallurgy as a Graduate Assistant in Physics, and at present is a candidate for the degree Master of Science, Physics Major.

After completion of the present work he is moving to Cape Girardeau, Missouri, where he has accepted a position as Instructor of Physics at Southeast Missouri State College.

